Thermal performance simulation of buildings' envelope with micro encapsulated Phase Change Materials (mPCMs)

Hongxia Zhou[1]*, *Anjan Rao Puttige*[1], *and Thomas Olofsson*[1]

[1]Applied Physics and Electronics (TFE), 90187 Umeå, Sweden

Abstract Wooden constructions are gaining popularity due to their economic benefits and their lower embodied CO_2 emissions. However, wood buildings face certain challenges, with one prominent issue being their limited thermal mass, resulting in lower thermal inertia within these structures. The scope of the study is to develop a simulation model in COMSOL Multiphysics (CM) to reflect the performance of buildings when PCMs are used in the structures. The model is validated with experimental data and then used to determine the optimal position of PCMs in a multi-layer wall, in addition, the optimal thickness of mPCMs has also been studied. The model in CM, representing a building with the shape of a box, consists of two versions. The first version (named as test box) is modelled with 5 sides of pure gypsum and 1 side of PCM-gypsum composite. The second version (named as reference box) is modelled with 6 sides of pure gypsum. These models are experimentally verified in the study. The study is focused on reducing the cooling load, the PCM gypsum composite material should function effectively during summer conditions in northern Sweden. A climate chamber is utilized to create temperature conditions of summer days in northern Sweden for the two boxes while performing measurements to validate the simulation model. Result indicates a slightly lower temperature value from CM in comparison to the experimental data. It also shows the optimized position of PCM layer is the internal surface of the room and the thickness is important to be considered depending on the location.

1 Introduction

The total quantity and area of buildings have grown rapidly resulting in increasing building energy consumption. The building energy consumption contribute to about 34% of global energy consumption according to international energy agency (IEA)[1]. Light-weight buildings are widely used due to their benefits like faster and cheaper during building process compared to other traditional building materials [2]. However, their low thermal inertia increases the fluctuation of energy load and air-conditioning when applied. IEA reported that the energy spent on air-conditioner for space cooling is around 20% of the total energy used in buildings. In Europe, the average annual air temperature has risen up to 1.7 ˚C above the pre-industrial level [3]. The cooling energy load is predicted to increase by 72% from 2015 to 2030 in Europe according to European Union [4].

One of the innovative methods to reduce the energy consumption of light-weight buildings is the development of passive design of buildings using latent heat thermal energy storage system. Phase change materials have been proved to be good materials that can store and release large amount of heat without large volume change. Several studies [5-7] have demonstrated that incorporating PCM into buildings may help refine the thermal comfort by lowering the temperature amplitude and shifting the peak temperature.

The building sector consumes 20%-40% of all generated energy, and about 50% of this energy is spent on heating, ventilation and air conditioning [8]. Wood buildings has gained interest in the past years with its advantages of fast construction, low cost, etc. However, the lower thermal mass limited of wood building has raised fear of large variations in indoor temperature that has limited the construction of wood buildings. The thermal mass of a building can be increased either by increasing the mass of the building envelope or by using PCM [9]. In addition, the application of PCM can reduce the heat transferred to and from the wood system and thereafter reduce the buildings energy consumption. When analyzing this issue, [10] indicated that it is effective to use PCM with peak melting temperatures of 23-24 °C in subarctic climate conditions.

For the application of PCM in wood buildings, the location of PCM has been studied by researchers [11-15]. However, this issue is still not resolved and requires further study and instruction, especially when subarctic climate is the condition. This study developed and validated a COMSOL model that can be used to predict the performance of PCM wall layers on the regulation of room temperatures.

2 Simulation tool

COMSOL Multiphysics 5.4 is used in this study for the simulation of PCM performance in building systems. The simulated model is an analogy of a representative

*Corresponding author: hongxia.zhou@umu.se

'building' model that has been studied in previous work [16]. The geometry of the model can be found in Fig.1, the green color stands for the PCM-gypsum wall side, while gypsum wall is marked with gray.

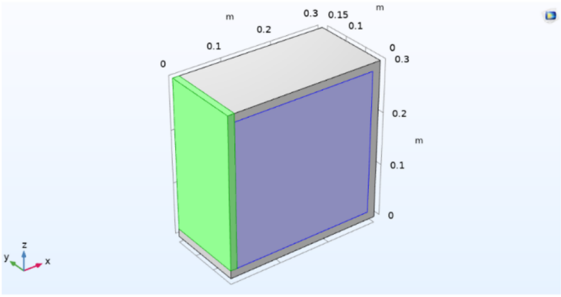

Fig.1 Geometry of the test box: PCM-gypsum composite wall in green, pure gypsum wall in gray and air domain in blue.

2.1 Governing equation

The numerical models of the study include physics of 'Heat Transfer in Solids' and 'Heat transfer in surface-to-surface' from COMSOL.

The heat transfer in solids and fluids is solved with Fourier's Law:

$$\rho c_p \frac{\partial T}{\partial t} + \rho c_p u \cdot \nabla T + \nabla \cdot q = Q + Q_{ted} \quad (1)$$

where the ρ denotes material density (kg/m3), c_p is specific heat (J/kgK), T is temperature(K), t is time (s), u is the velocity vector (m/s), q is the conductive heat flux (W/m^2), Q is any additional heat source (W/m^3) and $Q_{ted}$is the thermoelastic damping (W/m^3).

2.2 Initial and boundary conditions

The outdoor temperature used in CM was downloaded from the weather station database at TFE, Umeå University, consisting of the first three days of July in the summer of 2018. The data was chosen because it was the highest temperature in the last five years in Umeå. The measured data was averaged per hour so it had to be interpolated linearly in the simulation model first (see Fig.2), since the time step in CM was set to 1 minute. The initial temperature for all domains in the test box geometry was set to 17.62 °C, since the ambient air started at this temperature. This decreases the risk for numerical instability due to large temperature gradients in the area closest to the ambient air.

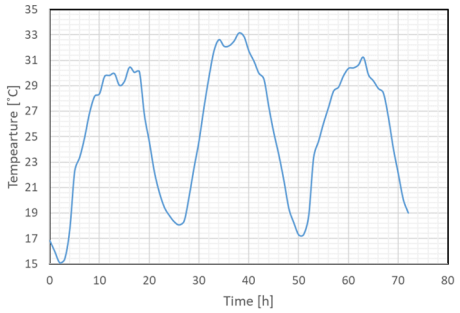

Fig.2 The linear interpolation of the hourly outdoor temperature measured at the first three days of July in Umeå Sweden 2018.

It shows in Fig.2 the highest temperature appears in the 2nd July with a value of about 32 °C, and the high temperature period (over 31 °C) lasted about 10 hours.

2.3 The heat transfer in solids and fluids interface

Most of the material properties for the pure gypsum and the PCM-gypsum composite, implemented in the simulation model, were obtained from the previous study by Zhou et al. [16]. In the study the thermal conductivities used for the exterior surfaces of the PCM gypsum composite and the pure gypsum were calculated using Eq. 2:

$$k = \frac{tq_{ext}}{T_{ext} - T_{int}} \quad (2)$$

where t is the thickness of the respective box wall type (m), T_{ext} is the exterior surface temperature (K), T_{int} is the interior surface temperature (K) and the convective heat flux q_{ext} (W/m^2) is calculated with the same heat transfer coefficient of 10 W/m^2K for both materials using Eq. (3)

$$q_{ext} = h(T_{amb} - T_{ext}) \quad (3)$$

where T_{amb} is the temperature in the climate chamber (K).

The resulting thermal conductivity of the PCM-gypsum composite, during solid-liquid transition, was inserted as an interpolation in the simulation model, as seen in Fig.3. The thermal conductivity peaks (0.65 $W/(m \cdot K)$) over temperatures corresponding to when the solid-liquid phase change occurs. Since there was no equivalent thermal conductivity data for liquid-solid transition, it is assumed to be the same as for solid-liquid transition, with a change to a 1.2 degrees lower temperature for during solidification process. This is the same temperature difference as between the phase transition temperatures of melting and solidification, also called sub-cooling degree. The average thermal conductivity for pure gypsum became 0.09 $W/(m \cdot K)$ for the test box and 1 $W/(m \cdot K)$ for the reference box. Subsequently, the thermal conductivity of each material was applied to the wall domains in the simulation model.

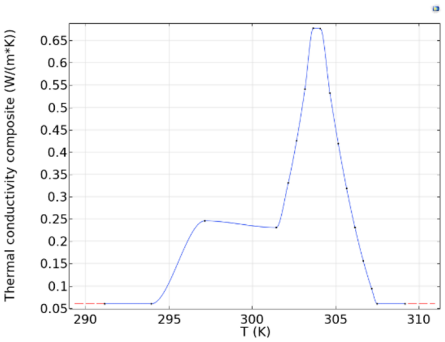

Fig.3 Thermal conductivity for the melting transition interpolated in COMSOL.

While the specific heat data of the PCM-gypsum composite board has been taken from previous study [16].

2.4 Surface to surface radiation interface

The Surface-to-Surface radiation interface is part of the Heat transfer module of CM. All the surfaces on the inside and on the outside of the test box (and reference box) were defined as diffuse. Ambient-to-surface radiation was included in the simulation model automatically when the outside surfaces were defined. By default, fluid domains are considered transparent and solid domains opaque, so the interior air domain and wall domains in between its surfaces did not need to be defined. The view factor to the ambient is zero inside the enclosure so there were separate view factors computed for the inside and outside. The ambient was represented by the climate chamber's interior walls, which implied that solar irradiance and long wave radiation could be neglected in the simulation model. The emissivity of the PCM-gypsum composite and the pure gypsum surfaces were both assumed to be 0.85 according to [17].

2.5 Temperature monitoring in the simulation and the mesh

The temperature evolution over time were monitored with boundary point probes at five different locations - the exterior and interior surfaces of one of the gypsum walls, the exterior and interior surfaces of the PCM-gypsum composite wall and at a point inside the interior air space. Temperature values at 1-minute intervals were obtained from the 72-hour time period.
Both a tetrahedral mesh and a swept mesh were used in the simulation. The swept mesh utilized the high aspect ratio of the hexahedral elements, allowing for a finer mesh size at the boundaries of the interior air domain where the larger air velocity gradients and temperature gradients occur and where two of the probes were located. Fig. 4 shows the tetrahedral mesh used for the entire test box on the left and the swept mesh (used for interior air domain) mixed with a tetrahedral mesh (used for walls) for the reference box on the right.

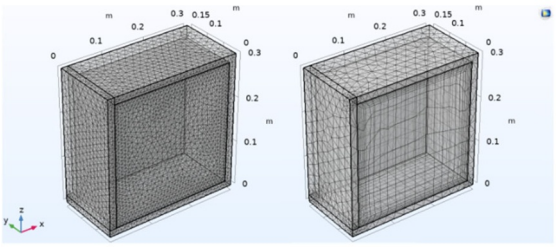

Fig. 4 The two different kinds of mesh used: fine tetrahedral mesh (left) and a mix of tetrahedral and swept mesh (right).

3 Experimental set-up

An experimental set-up discussed in [16] has been used for conducting experimental study. The dimension of boxes in experiment and simulation are 30 cm x 30 cm x 30 cm with an average wall thickness of 1.5 cm. The PCM-gypsum composite wall of the test box was slightly thinner with a thickness of 1.25 cm due to the inaccuracy from manufacturing process. The composite, which contains 30 vol% PCM and 70 vol% gypsum, was constructed according to Zhou et al. [18]. The other walls were made of 100% gypsum. T-type thermocouples, with an uncertainty of ±0.1K, were attached to the five different locations on the boxes corresponding to the boundary point probes in the simulation. The climate chamber used in the experiment was a Discovery MY from ASC, fitted with a fan to maintain uniform temperature throughout the $1m^3$ internal space. The two boxes were placed in the climate chamber, with the sensors connected. The climate chamber then generated a temperature profile according to Fig. 2, for the 72-hour duration of the measurement. Fig. 5 shows the test box placed in the climate chamber with a sensor attached to the PCM-gypsum composite wall.

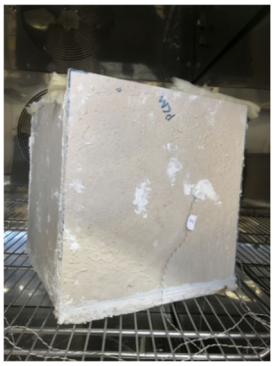

Fig. 5: The test box placed in a climate chamber with sensors attached.

3.1 Evaluation of simulation model

The model accuracy was checked with Root Mean Squared Error (RMSE) and the normalized RMSE (NRMSE). The metrics are indicators of how well the model can predict data, the lower the values the better prediction. RMSE is the most representative metric for

prediction accuracy [18]. A rule of thumb is that a RMSE less than 0.5 °C shows that the model can predict the data well, though in fact there exists no fixed threshold and it should be interpreted comparatively. The RMSE was calculated with Eq. (4):

$$RMSE = \sqrt{\frac{\sum(S-M)^2}{N}} \quad (4)$$

where S is the simulated value, M is the measured value, and N is the number of observations. By normalizing the RMSE with the range of the measured data, the RMSE can be evaluated relative to the dataset that it was created from. The NRMSE (%) was calculated by Eq. (5):

$$NRMSE = \frac{RMSE}{y_{max}-y_{min}} \times 100\% \quad (5)$$

where $y_{max} - y_{min}$ is the range of the measured data.

3.2 Layer sequencing and thickness specification of PCM-gypsum composite layer

A parametric study was performed in CM, with focus on how to improve the cooling effect of PCM on the test box during high ambient temperatures. The first part examined the effect from varying the placement of the PCM-composite layer in different sequences together with extruded polystyrene (EPS) layers, following the example described by Zhou et al. [18]. The gypsum in the other walls of the test box was replaced by EPS of the same thickness (1.5 cm) in order to create similar thermal conductivity in the entire envelope. The different configurations, with the PCM-gypsum composite layer highlighted in green, are illustrated in Fig. 6. The front wall consists of either two layers (2x1.5 cm) or three layers (3x1.5 cm). A PCM-gypsum composite layer was not included in the c and f configurations. To examine the effect of sequencing on the test box, the interior air temperature curves were analysed and compared to each other.

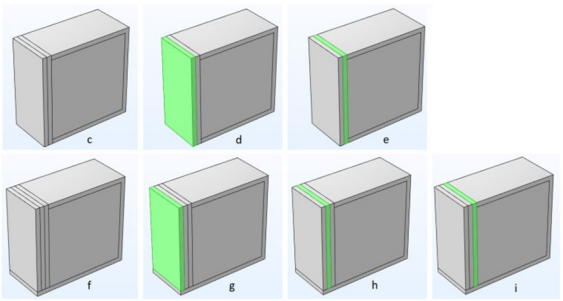

Fig.6 Configuration of the front wall: PCM-gypsum composite wall is indicated by the green layer.

The second part of the parametric study examined the effect of thickness of the PCM-gypsum composite layer on the interior air temperature variation. The configurations *d* and *e* with a PCM composite layer thickness of 1.5 cm in the previous part were compared to configurations where the thickness is increased to 3.0 cm and 4.5 cm for the outside position and inside position, respectively, as seen in Fig. 7.

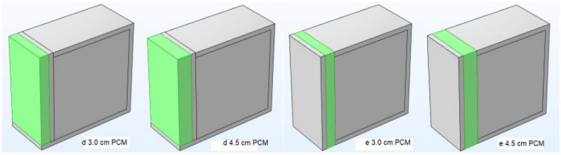

Fig. 7: Configuration of the front wall where the thickness of the PCM layer is changed: PCM-gypsum composite wall is indicated with green layer.

4 Results and discussion

Fig. 8 shows the temperature distribution at 10 hours from simulation. When the ambient temperature increases and the PCM is within its melting temperature range the PCM gypsum composite wall holds a lower temperature than the gypsum walls and interior air, indicated by the area marked in purple.

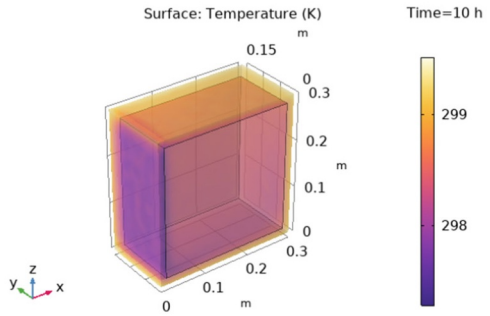

Fig. 8: Temperature distribution in 10 hours of test box, purple area is the PCM-composite wall.

The temperature variation in different locations has been derived from the CM simulation shown in Fig.9. It shows that with the increasing ambient temperature, the surface temperature on PCM also increases, and a phase transition appears when the external surface temperature is over 22 °C which is noticed as a slower increase of temperature followed by a sharp increase after transition is done.

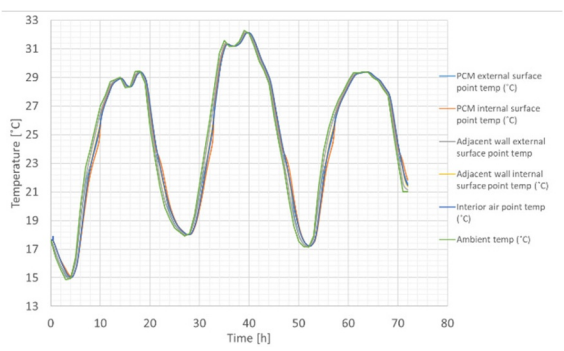

Fig. 9: Temperature in different locations derived from the simulation.

4.1 Comparing tetrahedral mesh and swept mesh

Using the tetrahedral mesh was slow but much easier to implement and can be adapted to almost any geometry. It was set to physics-controlled and the element size to fine. The number of DOF solved for was 177447 for the test box and 176036 for the reference box. The solution time was 19 hours and 17 minutes for the test box and 20 hours for the reference box. Implementing the swept mesh for the air domain increased the solution speed significantly. Tetrahedral mesh, of fine element size, was still used for the gypsum walls and PCM-gypsum composite. The mapped surface mesh was designed with 16 number of elements and an element ratio of 3, while the swept mesh was designed with the 8 number of elements and an element ratio of 3. The number of DOF solved for was 37890 for the test box and 37664 for the reference box. The solution time was 3 hours and 4 minutes for the test box and to 2 hours and 35 minutes for the reference box. The temperature curves resulting from using different mesh type for the PCM-gypsum composite exterior wall were compared, as seen in Fig. 10. The tetrahedral mesh with element size set to fine and the mixed swept/tetrahedral mesh gave very similar results. Thus, there were no disadvantages regarding accuracy in using the swept mesh on the interior air domain.

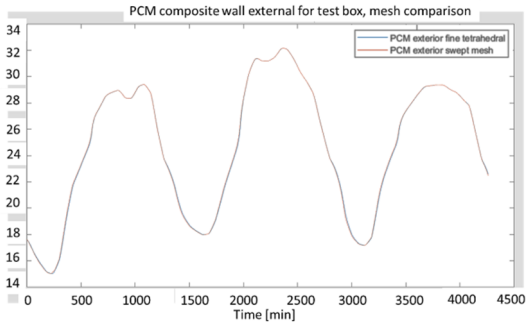

Fig.10: Temperature curves for PCM-gypsum composite exterior wall by using both mesh types.

The temperature curves for the interior air domain were also compared, as seen in Fig. 11, the tetrahedral mesh and the swept/tetrahedral mesh both showed numerical instability for the first hours.

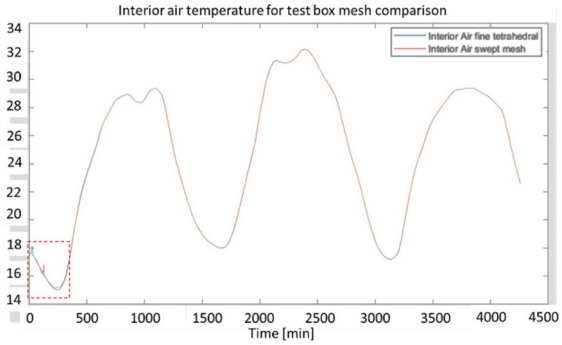

Fig. 11: Temperature curves for interior air domain for both mesh types

The convergence plots showed a very high reciprocal of step size at the beginning of the solving process for both solutions. Fig. 12 shows the convergence plot when using a tetrahedral mesh. The high reciprocal of step size could be due to that there is no movement or very little movement of the air at first, when the CFD module is set to laminar flow.

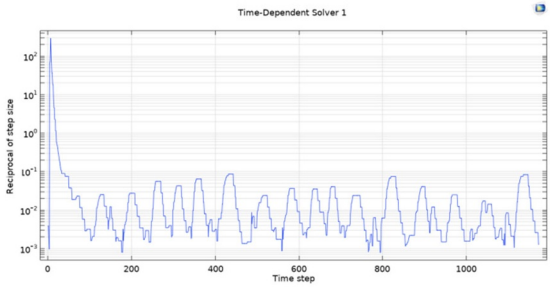

Fig. 12: The convergence plot for the simulation when tetrahedral mesh is used.

4.2 Validation of the simulation model by experimental data

The data attained from the 72-hour climate chamber run was measured in one second time step, so the values had to be averaged over 60 second intervals to make the comparison with the simulation values with output times for every minute. The ambient temperature curve from the simulated data was calibrated against the air temperature sensor in the climate chamber to get the timeline right. Temperature curves from using a tetrahedral mesh for the test box and reference box were used in the validation. The probe data from the numerical simulation were compared to the equivalent sensor data from the experimental measurements. Fig. 13 and Fig. 14 shows the experimental and simulated temperature curves for the gypsum exterior wall and the gypsum interior wall, respectively, for both test box and reference box. Both plots show consistently lower temperatures for the experimental measurements. The largest deviations appeared at the curve's peaks and valleys. One possible explanation is that the climate chamber was not able to create a uniform enough temperature distribution. However, the deviation on the interior walls should be relatively smaller in this case, which is not observed. The larger deviations on the interior walls could be caused by an error in sensor calibration.

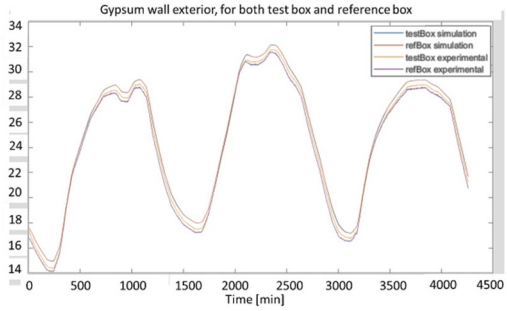

Fig.13: Temperature curves from experimental measurements and the numerical simulation on the exterior gypsum wall of both test box and reference box

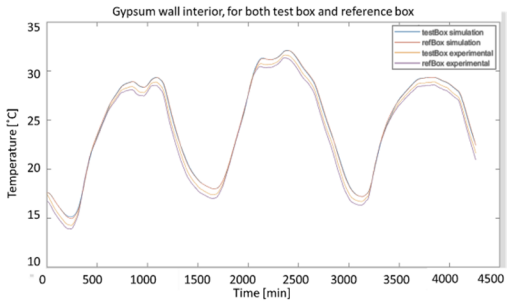

Fig. 14: Temperature curves from experimental measurements and the numerical simulation for interior gypsum wall of both test box and reference box

Fig. 15 and Fig. 16 show the PCM-gypsum composite walls exterior and interior surface. The interior PCM wall temperature shows better agreement between simulated and experimental values than the exterior PCM walls. The deviation was larger in PCM walls than the gypsum walls and the deviation is significant at the peaks and valleys. At the temperature interval where the PCM is activated, the simulated temperatures showed a rate of change with time very similar to the experimental equivalent i.e. they have the same slope in the transition temperature interval. This suggested that the PCM acts as it should in the simulation, with regards to latent heat storage. The deviation between simulated and experimental curves seemed to depend more on a systematically lower temperature in the chamber, as if it is always a few temperature degrees behind and it cannot catch up when reaching the peaks, because the chamber temperature is not reaching the prescribed temperature. The interior air temperature curves in Fig. 17 showed the least deviation between simulated and experimental values. According to Fig. 9, the temperature at all locations reached the ambient temperature at the peak at around 14 hours, there is not enough thermal mass built into the boxes, despite the PCM, to avoid that. The same thing occurred for all the peaks and all the valleys in the simulation - the curves were united at the ambient temperature. Assuming that this is true, it should have happened also in the experimental situation. But this is not observed, hence this supports our hypothesis that the chamber could not reach the highest prescribed temperature. Though for the interior air the peaks and valleys of the experimental curves ended up closer to the simulated curves than they had been in any of the other locations. The explanation could be that the wire of the temperature sensor was hanging freely in the interior air space and was not attached to the walls as the other sensors, which may have caused a lower thermal resistance between the air and the temperature sensor.

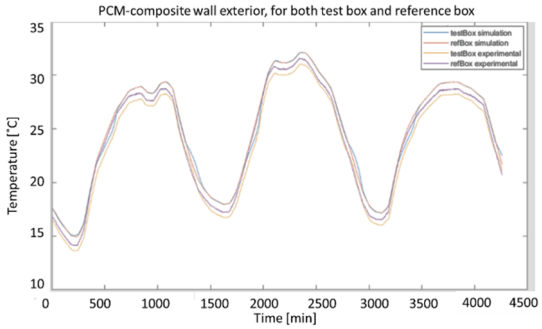

Fig. 15: Temperature curves from experimental measurements and the numerical simulation, from a point on the exterior PCM wall of the test box and the equivalent gypsum wall of reference box.

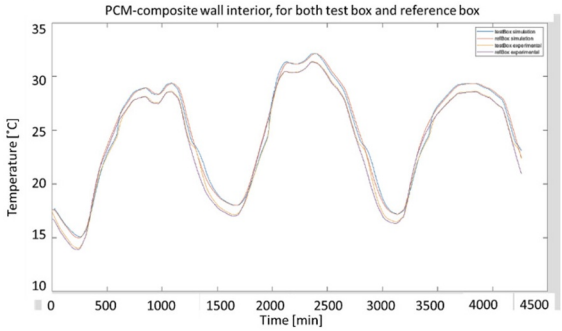

Fig. 16: Temperature curves from experimental measurements and the numerical simulation, from a point on the interior PCM wall of the test box and the equivalent gypsum wall of reference box.

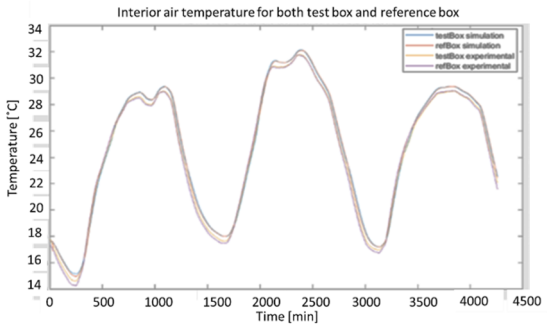

Fig. 17: Temperature curves from experimental measurements and the numerical simulation, from a point inside the air spaces of both test box and reference box.

The RMSEs and NRMSEs from the comparison of the numerical and experimental results are presented in Table 1. In the absence of data to compare with, the RMSEs were interpreted using the rule of thumb. The largest errors were 1.14 at the exterior surface of the PCM-gypsum composite wall for the test box and 0.94 for the gypsum wall interior surface (at the PCM wall position) of the reference box. The normalized RMSE

were just above 5% for the gypsum walls of the reference box and above 6% for the PCM exterior wall of the test box.

Table 1: RMSEs and NRMSEs of experimental and numerical results

	Gypsum External		Gypsum internal	
	Test	Ref	Test	Ref
RMSE/°C	0.41	0.68	0.56	0.93
NRMSE/%	2.4	3.9	3.2	5.3
	PCM external		PCM internal	
	Test	Ref	Test	Ref
RMSE/°C	1.14	0.68	0.76	0.94
NRMSE/%	6.5	3.9	4.5	5.4

4.3 Location specification

Seven different configurations of a PCM-gypsum composite layer and XPS layers, each of thickness 1.5 cm, were tested in CM with the validated simulation model, using the original ambient temperature curve. The interior air temperature curves for each configuration are plotted in Fig. 18. Looking closer at the first peaks of the curves in Figure 18, the configurations e, h, i showed significantly better properties. They were better at sustaining a lower interior temperature during the ambient temperature peak.

This suggested that configurations with the composite layer near to the interior air space are preferable during the cooling season, at least under the current circumstances i.e., they provided a better match between the transition temperature range of the PCM and the interior temperature of the test box during the unusually high ambient summer temperatures. The motivation to keep the PCM close to or on the external side would be better storage efficiency, but it was not possible to track the liquid fraction over time, so this indicator was not considered.

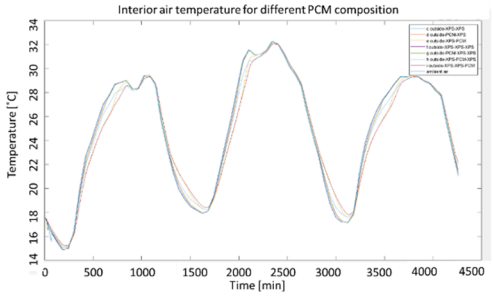

Fig. 18: Temperature curves for a point inside the air space from COMSOL for different wall configurations

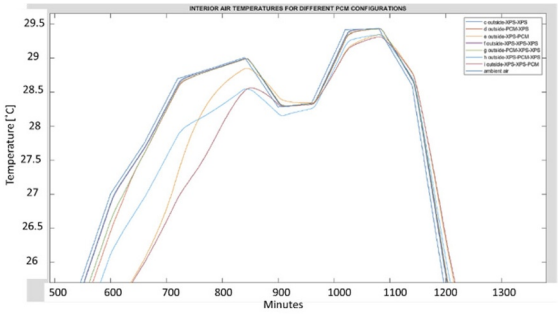

Fig. 19: A close-up of the first peak of temperature curves from Fig. 18.

4.4 Optimization of the thickness of PCM-gypsum composite layer

When the effect from changing the thickness of the PCM-gypsum composite layer were examined, as seen in Fig. 20. The figure shows the temperature variation inside the box with three different thicknesses of PCM-gypsum layer (1.5cm, 3.0 cm and 4.5 cm). It shows that putting a thickness of 4.5 cm layer next to the interior space (configuration *e*) was the best alternative for cooling, followed by the 3.0 cm PCM layer on the same position.

The third best alternative was not the thin PCM layer of 1.5 cm on the inside, but the very thick 4.5 cm PCM layer on the outside. Increasing the PCM layer thickness does not lead to a decrease in insulation material thickness, so the thermal conductivity in the front wall is not increased. But the storage capacity is most likely affected, with less complete phase change cycles, since thicker PCMs are difficult to recharge. The decreased storage efficiency should be weighed against the increased heat storage capacity when choosing the optimal thickness in real life but as mentioned, in this study, the liquid fraction was not tracked in the simulation.

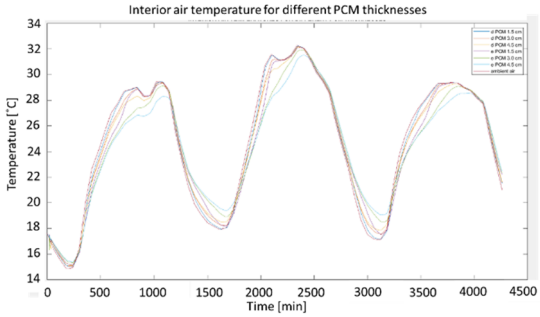

Fig. 20: Temperature curves for a point inside the air space for different PCM thicknesses.

5 Conclusion and discussion

A COMSOL Multiphysics model has been developed in this study for the simulation of building performance when phase change materials (PCM) are used. The developed model has been validated by experimental data. The simulation results indicate that for a severe

climate profile like Umeå Sweden, when PCM is used to regulate internal temperature, it's better to locate PCM as the internal surface than external surface. It also indicated that a 4.5 cm PCM placed as external surface is better than a 1.5 cm PCM places as internal surface layer.

A recommendation from this study is to create functions in the simulation model to predict the liquid fraction of PCM during the solid-liquid phase transition process.

Acknowledgement:

For financial support, the authors would like to acknowledge E2B2-Swedish Energy Agency project Phase Change Material to increase the thermal inertia of wooden buildings project number P2021-00248 and project DEVISE, ERA-NET Smart Energy Systems and Mission Innovation Joint Call 2019 (MICall19), Kempestiftelserna (JCSMK23-0121) and The China Ministry of Education International Cooperation Joined Laboratory.

References

1. https://www.iea.org/energy-system/buildings#tracking [Accessed 13 February 2024]
2. F. Asdrubali, B. Ferracuti, L. Lombardi, C. Guattari, L. Evangelisti, G. Grazieschi,A review of structural, thermo-physical, acoustical, and environmental properties of wooden materials for building applications,
   Building and Environment, 114 (2017)https://doi.org/10.1016/j.buildenv.2016.12.033
3. European Environment Agency. Global and European temperature. 2019. https://www.eea.europa.eu/data-and-maps/indicators/global-and-europeantemperature-9/assessment. [Accessed 13 February 2024]
4. International Renewable Energy Agency. Heating & cooling 2020. https:// www.irena.org/heatingcooling. [Accessed 27 February 2020].
5. Shi X, Memon SA, Tang W, Cui H, Xing F. Experimental assessment of position of macro encapsulated phase change material in concrete walls on indoor temperatures and humidity levels. Energy Build 2014;71:80e7. https:// doi.org/10.1016/J.ENBUILD.2013.12.001.
6. Rathore PKS, Shukla SK. An experimental evaluation of thermal behavior of the building envelope using macro-encapsulated PCM for energy savings. Renew Energy 2020;149:1300e13.
7. Hasan MI, Basher HO, Shdhan AO. Experimental investigation of phase change materials for insulation of residential buildings. Sustain Cities Soc 2018.
8. P. Marin, M. Saffari, A.D. Gracia, X. Zhu, M.M. Farid, L.F. Cabeza, S. Ushak, Energy savings due to the use of PCM for relocatable lightweight buildings passive heating and cooling in different weather conditions, Energy Build. 129 (2016) 274–283.
9. F. Guarino, A. Athienitis, M. Cellura, D. Bastien, PCM thermal storage design in building: Experimental studies and applications to solaria in cold climates, Applied Energy, 185 (2017) 95-106.
10. K. Nazir, S.A. Memon, A. Saurbayeva, A. Ahmad, Energy consumption predictions by genetic programming methods for PCM integrated building in the tropical savanna climate zone, J. Build. Eng. 68 (2023). 106115.
11. S. Liu, J. Wang, Li Meng, C. Hu, X. Meng, Location of the phase-change material (PCM) layer on thermal performance of light-weight walls, Int. J. LowCarbon Technolog. (2023) ctac096.
12. X. Jin, M.A. Medina, X. Zhang, On the importance of the location of PCMs in building walls for enhanced thermal performance, Applied energy. 106 (2013)72–78.
13. X. Jin, S. Zhang, X. Xu, X. Zhang, Effects of PCM state on its phase change performance and the thermal performance of building walls, Building and Environment. 81 (2014) 334–339.
14. X. Jin, M.A. Medina, X. Zhang, Numerical analysis for the optimal location of a thin PCM layer in frame walls, Appl. Therm. Eng. 103 (2016) 1057–1063.
15. X. Jin, D. Shi, M.A. Medina, X. Shi, X. Zhou, X. Zhang, Optimal location of PCM layer in building walls under Nanjing (China) weather conditions, Journal of Thermal Analysis and Calorimetry. 129 (3) (2017) 1767–1778.
16. H. Zhou, A.R. Puttige, G. Nair, T. Olofsson, Experimental study of micro-encapsulated phase change materials' influence on indoor temperature, Journal of Physics : conference series 2023.
17. Engineeringtoolbox.com. Engineering toolbox. [online]. (Accessed May 2023). URL https://www.engineeringtoolbox.com/.
18. H. Zhou, Å. Fransson, T. Olofsson, An Explicit Finite Element Method for Thermal Simulations of Buildings with Phase Change Materials, Energies 14(19), 2021, special issue: Energy Performance, Management and Recovery in Buildings.